COMPARISON OF METHODOLOGIES FOR ASSESSING THE RISKS FROM NUCLEAR WEAPONS AND FROM NUCLEAR REACTORS*

Allan S. Benjamin
Sandia National Laboratories
P.O. Box 5800, M/S 0405
Albuquerque, New Mexico 87185
(505)845-8418

ABSTRACT

There are important differences between the safety principles for nuclear weapons and for nuclear reactors. For example, a principal concern for nuclear weapons is to prevent electrical energy from reaching the nuclear package during accidents produced by crashes, fires, and other hazards, whereas the foremost concern for nuclear reactors is to maintain coolant around the core in the event of certain system failures. Not surprisingly, new methods have had to be developed to assess the risk from nuclear weapons. These include fault tree transformations that accommodate time dependencies, thermal and structural analysis techniques that are fast and unconditionally stable, and parameter sampling methods that incorporate intelligent searching. This paper provides an overview of the new methods for nuclear weapons and compares them with existing methods for nuclear reactors. It also presents a new intelligent searching process for identifying potential nuclear detonation vulnerabilities. The new searching technique runs very rapidly on a workstation and shows promise for providing an accurate assessment of potential vulnerabilities with far fewer physical response calculations than would be required using a standard Monte Carlo sampling procedure.

INTRODUCTION

One of the main differences between nuclear weapons and nuclear reactors is that a nuclear weapon relies upon passive or inactive systems to ensure safety, while a nuclear reactor depends upon active systems for safety. In addition, a principal concern for nuclear weapons is to prevent electrical energy from reaching the nuclear package, whereas the foremost concern for nuclear reactors is to maintain coolant around the nuclear core. Thus many nuclear weapon risk assessments focus upon the conditions that could lead to new and unwanted electrical pathways, whereas nuclear reactor risk assessments focus upon conditions that could interrupt existing pathways for fluid flow.

Not surprisingly, while the methods that have been developed to assess the risks from nuclear reactors can be used for nuclear weapons, they are not always applied in the same way. Furthermore, new methods have had to be developed for certain aspects of probabilistic risk assessments (PRAs) for nuclear weapons that are not common to PRAs for nuclear reactors.

Methodologically, many of the differences between the two kinds of risk assessment can be characterized by differences in the nature of the failure regions. Risk assessments for nuclear reactors, and most other risk assessments, involve semi-infinite failure regions. For example, an assessment of the frequency of reactor core damage leading to possible meltdown involves determination of whether water can be provided to the reactor core before the core becomes uncoolable. If the amount of time without cooling is less than the critical time, core damage is arrested; if not, melting ensues. Similarly, risk assessments of plutonium dispersal for a nuclear weapon involved in a fire or a crash involve determination of whether the duration of the fire or the speed of the impact exceeds a critical value that may be a function of other variables, such as fire temperature and impact direction. Dispersal is assumed to result any time that the critical value is exceeded.

There is a class of risk assessment problems for nuclear weapons, however, that involves the determination of "failure islands." These center around the assessment of certain inadvertent nuclear detonations resulting from a fire, crash, or other physical hazard. For these problems, certain components of the system must fail in order to produce or allow unwanted electrical pathways, while others must survive in order to

* This work was supported by the United States Department of Energy under Contract DE-AC04-94AL85000.

propagate the signal. In modern safety designs, the former are called "strong links" and the latter "weak links." (Actually, the terms "strong link" and "weak link" imply a set of very stringent design and operational requirements which we will not elaborate upon, since they do not apply to the present discussion.)

To illustrate the nature of failure islands, a particular pathway leading to the undesired outcome might involve failure of a switch (strong link) to remain open, combined with survival of a capacitor (weak link) that is needed to store electrical energy. A fire or crash that is too severe would cause both the switch and the capacitor to fail, whereas one that is too benign would cause neither to fail. The failure region therefore involves environments of intermediate severity and very precise orientation with respect to the weapon system.

Figures 1 and 2 illustrate schematically the difference between semi-infinite failure regions and failure islands. In Figure 1, which simulates a nuclear reactor accident, Scenario 1 occurs if there is a particular accident initiator (AI_1) followed by two individual subsystems failing to operate (S_1 and S_2). Each subsystem becomes inoperable when certain parameter thresholds are exceeded. Scenario 2 involves a different accident initiator and set of system inoperabilities, which are left undefined in the figure. The overall parameter space is divided into a failure region (shaded) and a region of nonfailure (unshaded) by a boundary, or limit state, that is defined by the unions and intersections of the various thresholds.

In Figure 2, which simulates an inadvertent nuclear detonation accident, the scenarios are defined by races between strong links and weak links, rather than by individual subsystem failings. Scenario 1 occurs if there is a particular accident environment (AE_1) followed by the failing of each of two strong links (SL_1 and SL_2) before the failing of either of two weak links (WL_1 and WL_2). Scenario 2 is similarly defined in terms of a different accident environment and set of races. Each scenario produces one or more separate failure islands, which are indicated by shaded areas in the figure.

The differences in the nature of the failure regions make it necessary to adopt somewhat different approaches for the risk assessment. To mention a few before elaborating later, both nuclear reactor and nuclear weapon risk assessments use event trees and fault trees to describe the progressions of events and combinations of faults that could lead to undesired outcomes. However, nuclear reactor assessments usually result in a number of fault trees that feed into a single event tree, whereas nuclear weapon assessments usually involve the opposite. The fault tree for a nuclear weapon assessment tends to be larger than the fault tree for an individual system or component in a nuclear reactor, since the weapon application involves consideration not only of the parts of the system that must fail to produce unwanted electrical pathways, but also the parts that must not fail in order to propagate the signal. Furthermore, the fault tree may be time-dependent, because during postulated accidents involving nuclear

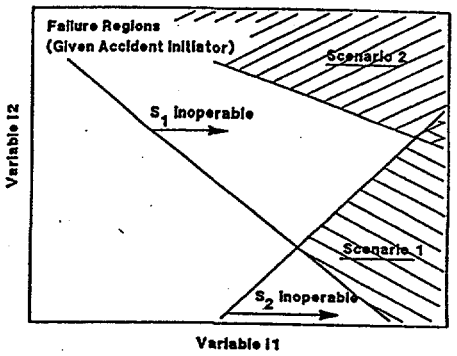

FIGURE 1. SCHEMATIC OF FAILURE REGIONS IN NUCLEAR REACTOR RISK ASSESSMENT.

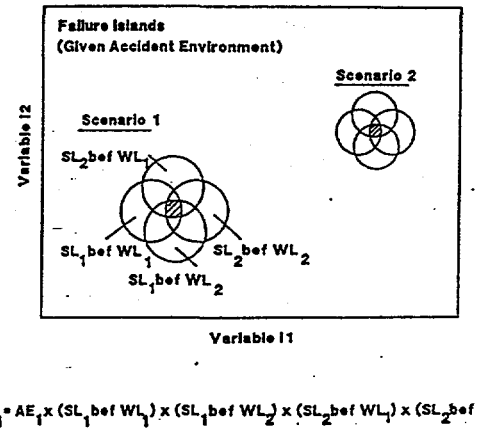

FIGURE 2. SCHEMATIC OF FAILURE ISLANDS IN NUCLEAR DETONATION RISK ASSESSMENT.

weapons, unwanted electrical pathways may exist only for limited time windows.

Because of these and other considerations, nuclear weapon risk assessments have spawned the development of a number of codes that are not typically required for nuclear reactor risk assessments. These include: (1) time-sensitive fault tree solution codes to track the existence of time-dependent vulnerabilities; (2) fast-running thermal and structural response codes, based on lumped element, spring-mass, and/or neural network approaches, to calculate the state of the system as a function of time for a large variety of possible fires and impacts; and (3) directed parameter sampling codes to facilitate the search for regions of the parameter space where electrical pathways may develop.

This paper provides an overview of the methods used for assessing risks from nuclear weapon, compares them with the

methods used for nuclear reactor assessment, and describes the new algorithms that have been developed in the areas enumerated above.

METHODOLOGY COMPARISON

Time-Sensitive Fault Trees

In risk assessments for nuclear detonation, event trees are used to define the abnormal environments that the weapon system could be exposed to, and fault trees are used to delineate the pathways that could lead to nuclear detonation. Quite often, a single fault tree is constructed in which the top event is the appearance of electrical energy at the detonators, and the lower level events include a combination of preexisting conditions, spurious failures, and component responses to the environment. Event trees are used to identify the environments and assess their frequencies, and physical response codes are used to evaluate the component responses.

Figure 3 illustrates portions of three types of cut sets (i.e., pathways) that could emanate from a risk assessment of nuclear detonation. The first is composed of a set of preexisting conditions resulting from human error (incorrect setting) and from the appearance of electrical energy. It should be noted that precautions against strong links being incorrectly set are so rigorous that the probabilities of these cut sets are predicted to be extremely low.

The second cut set provides an example of a preexisting condition (electrical energy) together with the occurrence of a highly directed abnormal environment (impact) which causes a set of critical components (strong links) to fail while another set (weak links) survives. It should be noted that design provisions

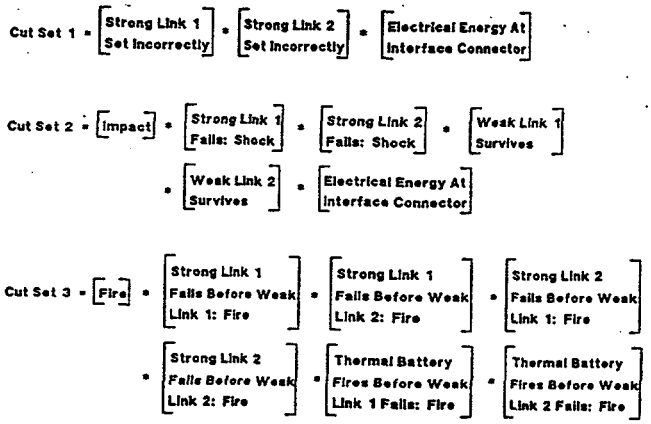

FIGURE 3. PORTIONS OF REPRESENTATIVE CUT SETS FROM NUCLEAR DETONATION RISK ASSESSMENTS.

for nuclear weapon systems embodied in modern safety themes make it extremely unlikely that a combination of strong link failures and weak link survival could occur in any credible abnormal environment.

The third cut set similarly involves responses of the components, but the abnormal environment is a fire rather than an impact. Unlike the responses to impacts, which occur over milliseconds, the responses to fires may occur over hours. Thus, the state of the system may change over time so that windows of vulnerability last long enough for the electrical system to become charged and capable of delivering energy to the detonators. To accommodate this time sensitivity, the portions of the cut sets dealing with responses to fires are transformed so that the base events represent races between pairs of components, rather than the states of individual components. For the undesired event to occur, each race involving a strong link or (in this case) an electrical source and a weak link must be lost. That is to say, each term in cut set 3 of Figure 3 must be "true."

In a typical nuclear detonation risk assessment, many thousands of cut sets are generated, and they typically involve combinations of the types of events illustrated in the three examples. The key difference between the nuclear weapons fault tree and the typical fault trees from nuclear reactor applications is the transformation from single to paired events in order to capture the time sensitivity of the state of the system.

PRA-Compatible Physical Response Analysis

Generally speaking, the number of physical response calculations that must be performed is much greater for problems that involve failure islands than for those that involve semi-inifinite failure regions. In the former case, the analyst must find a large number of isolated success or failure boundaries, whereas in the latter case, it is usually necessary to locate only one boundary.

A risk assessment involving a semi-infinite failure region typically requires on the order of tens or hundreds of physical response calculations, whereas a risk assessment involving many failure islands may require thousands or tens of thousands of calculations. For problems involving semi-infinite failure regions, there is a need for two levels of physical response modeling, which we refer to as very detailed and moderately detailed. For failure island problems, a third level of modeling is required, which we call minimally detailed.

For the very detailed physical response modeling, we are driven by present practice and past successes to finite-element modeling. Fine-mesh finite-element models are a proven method for determining accurate physical response predictions for complex systems. A very detailed thermal response model would typically involve meshing of the system into thousands to tens of thousands of finite elements. An analogously detailed structural

response model would typically require tens of thousands to hundreds of thousands of finite elements.

For the moderately detailed physical response modeling, we use "lumped mass" models and recurrent neural network models. One could also utilize coarse-meshed finite-element models in this context, but these have proven to be comparatively less useful as the coarseness increases because finite-element codes do not tend to be as stable or as fast running as lumped mass and neural network codes.

Lumped mass models are so named because the mass of each finite element is considered to be concentrated at a point. Subject to this simplification, they solve equations of heat transfer or motion that are similar to those solved in finite-element codes. The masses in a thermal model are thought of as being connected by thermal resistors, whereas the masses in a structural model are considered to be connected by mechanical springs. A lumped mass thermal response model would typically contain hundreds of masses, whereas a lumped mass structural model would more likely contain thousands. Lumped mass models have proven to be useful as estimators of the physical response of complex systems, particularly when they contain parameters that can be adjusted in order to calibrate them to the very detailed models.

A neural network model does not solve the governing physical response equations of the system, but relies completely upon the calibration, or training, of parameters in the network to achieve agreement with the very detailed models. A recurrent neural network model simulates a few key measures of the response of a thermal or structural system in a time-marching sense, by using the values of the response variables at the current time as inputs to determine the values one time step in the future.

For the minimally detailed physical response models, we typically use correlations based on response surface analysis or, alternatively, nonrecurrent neural networks. Nonrecurrent networks do not simulate the time-dependent behavior of a system as do recurrent networks, but instead directly predict the end state starting from the description of the system and the initial and boundary conditions. We use the minimally detailed models as screening tools to eliminate cases that most likely produce harmless responses with minimal time expenditure.

Following are brief descriptions of two lumped-mass computer codes we developed to evaluate the responses of complex systems to thermal and mechanical environments in a very efficient manner.

TEMPRA, an acronym for Thermal Evaluation and Matching Program for Risk Applications,[1] calculates the temperature responses of components in a system accounting for thermal conduction, convection, and radiation between elements and chemical reaction and/or phase change within elements. It uses a lumped element model with an unconditionally stable, semi-implicit, differential equations solver so that large time steps may be employed. The nonlinear differential equations of heat transfer are fully linearized before reduction to numerical form. Typically, a TEMPRA model utilizes approximately 500 to 1,000 lumped elements to model the response of a system where finite element models might use more than 10,000 elements. The accuracy of TEMPRA is enhanced by "benchmarking" its results against a set of finite-element results, which are presumed to have been benchmarked against experimental data. TEMPRA gains accuracy by the use of "adjustable constants," whose values are determined by a least-squares regression in order to compensate for the errors produced by mesh coarseness and mass lumping.

A problem that requires 24 hours of central processor unit (CPU) time using a detailed finite-element code on a SPARC-10 workstation typically requires about 10 minutes of CPU time using TEMPRA on the same platform.

STRESS, an acronym for Spring-mass Transient Response Evaluation for Structural Systems,[2] was developed for rapid evaluation of nonlinear dynamic responses to impacts and punctures. The code starts from a geometric representation of a structural system, such as the "patch" or "hyperpatch" geometry produced by the code PATRAN,[3] but instead of meshing the geometry in the conventional finite element sense, it converts it to a 3-D mesh composed of masses connected by springs. Like finite element codes, it calculates deformations, accelerations, stresses, and strains. The models in the code include nonlinear stiffnesses, material rupturing, and surface contact between initially disjoint components. The STRESS code contains a few adjustable constants to facilitate calibration of its results to finite-element code results or to experimental data. The calibration process is not automated as it is in the TEMPRA code, however, because the more oscillatory nature of the response in a structural system makes it more difficult to automate the process.

In a recent application, STRESS required about 40 minutes of CPU time on a CRAY-YMP computer to solve a problem that required about 40 hours using a detailed finite-element code.

Directed Parameter Sampling

In order to locate failure regions and determine probabilities of occurrence, it is necessary to sample the parameters that govern the problem. In a risk assessment, the parameters that are sampled may include the initial and boundary conditions imposed on the system, failure thresholds, and certain modeling parameters, such as material properties. Typically, sampling may be performed on several tens of parameters, which are assumed to be random variables with prescribed probability distributions. When completed, the products of a risk assessment often include a probability distribution for the frequency of an undesired outcome and an identification of the subregions of the parameter space that are associated with that outcome.

Like the choice of physical response analysis methods, the requirements on parameter sampling and probability determination differ according to the type of performance or risk assessment being performed. In nuclear reactor risk assessments

involving semi-infinite failure regions, a modified Monte Carlo procedure, called Latin hypercube sampling,[4] is frequently used both to sample the parameters and to determine the resultant probability distribution for the outcome. This method has worked well, but it can be inefficient for problems requiring many time-consuming physical response calculations, such as for risk assessments involving failure islands with low probability of occurrence. To address the question of nuclear weapon accidents that could lead to nuclear detonation, we have developed an intelligent searching algorithm called SEARCH to speed the rate of convergence.

The term "intelligent searching" is used to connote a process in which we sample the parameter space in an iterative fashion, with each iteration utilizing the results of previous iterations to improve the search. For the first iteration, the parameter space is sampled in a completely unbiased fashion, such as by random selection or by uniform canvassing of the space. For each sample member, we compute the physical response of the system using a risk-compatible physical response code such as TEMPRA or STRESS.

The results of the first iteration are used to develop an estimator that is capable of approximating the physical response of the system to new sets of environmental conditions. In the second iteration, the estimator is used to screen out conditions where there is virtually no chance of a vulnerability, so that the next set of physical response computations may be performed closer to the more meaningful regions. The required properties of the estimator are that it be very rapid and that it possess the characteristic of becoming increasingly accurate after each iteration.

USE OF INTELLIGENT SEARCHING IN NUCLEAR WEAPON SAFETY ASSESSMENTS

Synopsis of the Method

In assessments of the potential for inadvertent nuclear detonation, we focus upon a quantity we call "closeness to occurrence." Roughly speaking, this quantity represents the ratio of the peak response of the system to the response that would be required to produce a vulnerability. For a thermal system, we define closeness in terms of races between components. The closeness of a race between Components A and B is expressed mathematically as follows:

$$K_{A,B} = \frac{T_{pk,A}(t_{fl,B}) - T_{in}}{T_{fl,A} - T_{in}} \qquad (1)$$

where $t_{fl,B}$ is the failure time for Component B or the final time in the computation, whichever comes first; $T_{pk,A}(t_{fl,B})$ is the peak temperature achieved by Component A up to time $t_{fl,B}$; $T_{fl,A}$ is the failure temperature for Component A; and T_{in} is the initial temperature in the system. The race between A and B is lost, in the sense of Figures 2 and 3, if and only if $K_{A,B} \geq 1$. A vulnerability occurs when the race between A and B is part of the definition of a cut set leading to the undesired outcome. In simple mathematical terms, the overall closeness to occurrence for a cut set Z may be represented as follows:

$$K_Z = \min_{A,B \in Z} (K_{A,B}) \qquad (2)$$

where $A,B \in Z$ denotes that A and B are both members of Z.

With this definition in hand, we may summarize the principal steps in the intelligent searching process for nuclear weapon system vulnerabilities resulting from thermal environments. (The steps for structural systems are analogous.) The procedure, which is outlined in Figs. 4 through 6, is incorporated into our SEARCH computer code:

1. In the first iteration, a coarse hypercube of the input parameter space is set up and a physical response computation is made at each "corner" of the hypercube using TEMPRA (see Fig. 4a).

2. Before developing an estimator, the temperature responses are divided by the fire temperature and the time scales are multiplied by the fourth power of the fire temperature. This normalization of the primitive variables enables us to incorporate our preknowledge of the first-order response characteristics of the system. For example, the time for a component to achieve a certain level of temperature is inversely proportional to the radiative heat flux from the fire to the system as a whole, and the latter is proportional to the fourth power of the fire temperature over the range of temperatures of interest in the risk assessment.

3. Using the results from Steps 1 and 2, an estimator in the form of a response surface is developed for each of the following measures of response: (a) the normalized peak temperature achieved by each component during the accident scenario, and (b) the normalized times to reach various fractions of the peak temperature (see Fig. 5a,b). Taken together, these responses approximate the total temperature-time history for the component. The response equations can be viewed as truncated Taylor series and the coefficients in the response equations as the first-order partial derivatives of the responses with respect to each of the input variables together with all the associated cross derivatives (see Fig. 5c).

4. A very finely divided hypercube of the same parameter space is set up (see Fig. 4b), and the component responses are estimated for each intersection point using the response surfaces derived in Step 3. For each point, the estimations of component physical response are used to determine race closenesses using

(a) Physical Response Runs (Denoted by Circles)

(b) Sampling Points (Denoted by Intersections)

(Example for 3 Input Parameters)

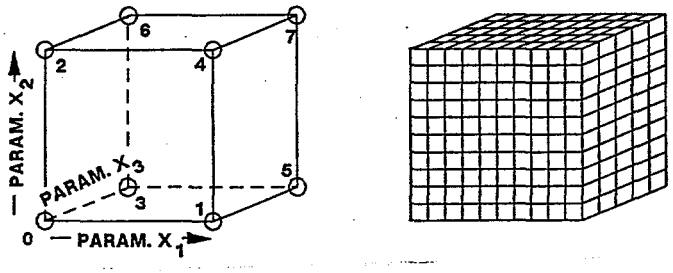

FIGURE 4. SCHEMATIC OF PARAMETER HYPERCUBE, INITIAL PHYSICAL RESPONSE COMPUTATIONS, AND ESTIMATOR SAMPLING MATRIX

(a) Thermal Response

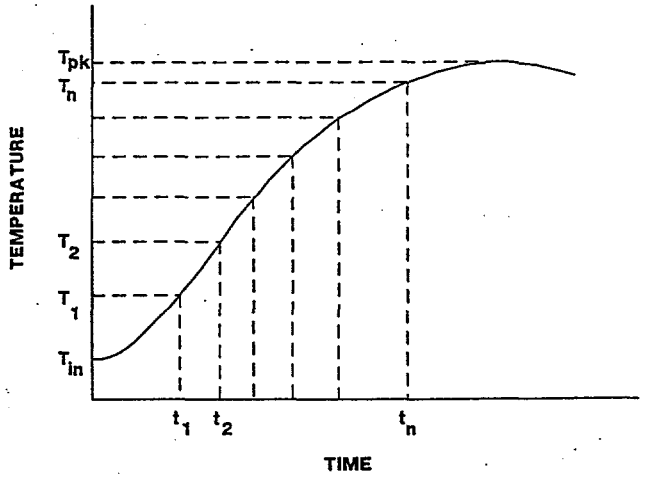

(b) Response Parameters:

$$Y_1 = \frac{T_{pk} - T_{in}}{T_{fire} - T_{in}} \qquad Y_{i+1} = t_i \frac{T_{fire}^4 - T_{in}^4}{T_{in}^4} \quad (i = 1,2,\ldots,n)$$

(c) Response Equation (Example for 3 Input Parameters)

$$Y_i = C_{0,i} + C_{1,i}\Delta X_1 + C_{2,i}\Delta X_2 + C_{3,i}\Delta X_3 + C_{4,i}\Delta X_1\Delta X_2 + C_{5,i}\Delta X_1\Delta X_3 + C_{6,i}\Delta X_2\Delta X_3 + C_{7,i}\Delta X_1\Delta X_2\Delta X_3$$

FIGURE 5. SCHEMATIC OF COMPONENT THERMAL RESPONSE, RESPONSE PARAMETERS, AND RESPONSE SURFACE EQUATION FORM

Equation (1), and the race closenesses are used to estimate the overall closeness to occurrence for each cut set using Equation (2).

5. The results from Step 4 are then binned according to user prescription (see Fig. 6a). Each bin represents a subset of the total parameter space, defined so as to encompass physically similar situations. For each bin, the boundaries of any islands of vulnerability are determined by inspection of the estimates obtained in Step 4, and the location of the center of the island is similarly estimated.

6. The results from Step 5 are evaluated to determine which potential islands of vulnerability are most credible and which parameters are most important for that particular vulnerability. (The importance of a parameter is defined here as the relative sensitivity of the closeness to occurrence to variations in that parameter.) Based on these findings, a number of estimated island centers are selected for further analysis (see Fig. 6a).

7. For each island center selected in Step 6, a subspace is defined in which the less important parameters are held at fixed values while the more important ones vary over their defined ranges. The subspace is then partitioned in such a way that the estimated island center becomes the common point of generation for the partitions (see Fig. 6b).

8. New physical response computations are performed at corners of the partitions for which a physical response computation has not previously been performed. Based on these new computations, a new set of response surface equations is developed for each partition.

9. Steps 4 and 5 are repeated for each new partition, using the new response surface equations developed in Step 8. If the results from Step 6 are notably different from the previous iteration, the iterative process is repeated starting from Step 6.

Example Results

We applied the intelligent searching method described above to an idealized model of a nuclear weapon system to investigate the convergence properties and computational efficiency of the method. The safety design of the system consisted of six components, designated as strong links A_1, A_2, A_3, and weak links B_1, B_2, B_3. Each had a different temperature threshold beyond which the component was assumed to fail.

We considered two cut sets, or levels of vulnerability. The first consisted of the responses of Components A_1, A_2, B_1, and B_2, whereas the second included all the components. The problem included eight input variables which are summarized in Table 1. They described the configuration of the weapon system, the way that the fire was oriented to it (i.e., patterns of exposure and sheltering on four circumferential quadrants), the thermal models for an internal material and for the external sheltering medium, and the fire temperature.

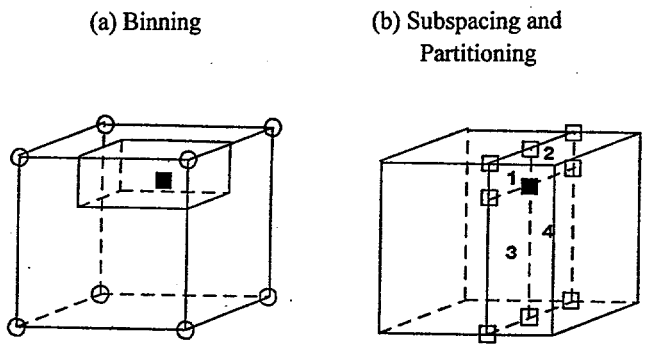

FIGURE 6. SCHEMATIC OF BINNING, SUBSPACING, AND PARTITIONING

Some of the results are shown in Figs. 7 and 8. Each figure depicts a cut through the parameter hypercube in which the variation of the overall closeness to occurrence with fire temperature is shown with all other variables held constant. Both figures exhibit the occurrence of local peaks, which represent potential failure islands if the overall closeness is greater than or equal to 1.0. Each peak, or failure island, is associated with a critical race between a strong link and a weak link. The discontinuity in slope at a peak is caused by a transition in the weak link response. At fire temperatures below the point where the peak occurs, the weak link reaches a steady-state temperature that is lower than its failure temperature. At higher fire temperatures, the steady-state weak link temperature is higher than its failure temperature.

TABLE 1. EXAMPLE PROBLEM PARAMETERS

1. System configuration	a. Reentry vehicle (RV) b. Shipping, endplates on c. Shipping, endplates off
2. Exposure for 1st quadrant	a. Engulfed in fire b. Shielded by immersion
3. Exposure for 2nd quadrant	a. Engulfed in fire b. Shielded by immersion
4. Exposure for 3rd quadrant	a. Engulfed in fire b. Shielded by immersion
5. Exposure for 4th quadrant	a. Engulfed in fire b. Shielded by immersion
6. Thermal model for internal foam	a. Radiation-based b. Conduction-based
7. Heat transfer coefficient for immersing medium	0.0 to 0.2 BTU/ft^2-s-°F (uniformly continuous)
8. Fire temperature	1000 to 5000 °F (uniformly continuous)

In the first iteration, we performed 124 thermal response computations with the TEMPRA code to cover the most significant corners of the parameter hypercube and to develop the response surface equations. Two of these runs happened to fall within the cut of Fig. 7, whereas none appeared in the cut of Fig. 8. We then applied the resulting response equations at approximately 150,000 points in the hypercube to estimate the responses of the system to a wide spectrum of parameter variations. In subsequent iterations, we partitioned the temperature scale at the most significant local peaks and performed a few additional TEMPRA calculations as indicated in the figures.

It may be seen that only two iterations were required for the method to converge quite closely to the correct location and peak value of the principal failure island of Fig. 7, whereas three iterations were required for the same result in Fig. 8. We verified that the code had converged to the correct values by performing an additional set of TEMPRA runs in order to obtain the solid curve in each figure.

From the results obtained so far, the intelligent searching process appears to be able to characterize the failure islands of the example problem quite accurately with approximately one-tenth as many physical response calculations as would be

required by a random sampling process without the benefit of intelligent searching. The amount of CPU time required for the entire search, exclusive of the TEMPRA calculations, was only about 30 minutes on a SPARC-10 workstation.

CONCLUSIONS

Risk assessments for inadvertent nuclear detonation in nuclear weapon systems utilize many of the same tools as nuclear reactor risk assessments. However, the differences between the designs of the systems have made it necessary to develop new techniques in the following areas: (1) time-dependent fault trees, (2) fast-running thermal and structural numerical simulations, and (3) parameter sampling utilizing intelligent searching. The approach for intelligent searching described in this paper has the potential for locating nuclear detonation vulnerabilities of very low probability and appears to require far fewer time-consuming physical response computations than standard sampling methods. The results indicate that the process should scale well with increasing size and complexity of a problem.

REFERENCES

1. A. S. Benjamin, R. Beraun, N. N. Brown, and M. P. Sherman, "Evaluation of Conductive, Radiative, Chemical, and Convective Heat Transfer in Complex Systems Using a Fast-Running, Implicit, Lumped Capacitance Formulation," *Proceedings of the ASME National Heat Transfer Conference*, Portland, OR, August 1995.

2. A. S. Benjamin, B. S. Altman, and J. D. Gruda, "Evaluation of Nonlinear Structural Responses Using a Fast-Running Spring-Mass Formulation," *Proceedings of International Conference on Computational Engineering Science*, Mauna Lani, HI, July 1995.

3. PATRAN Division, 1992, "P3/PATRAN User Manual," Publ. No. 903000, PDA Engineering, Costa Mesa, CA.

4. R. L. Iman and M. J. Shortencarier, "A FORTRAN 77 Program and Users Guide for the Generation of Latin Hypercube and Random Samples for Use with Computer Models," NUREG/CR-3624, SAND83-2365, Sandia National Laboratories, Albuquerque, NM, 1984.

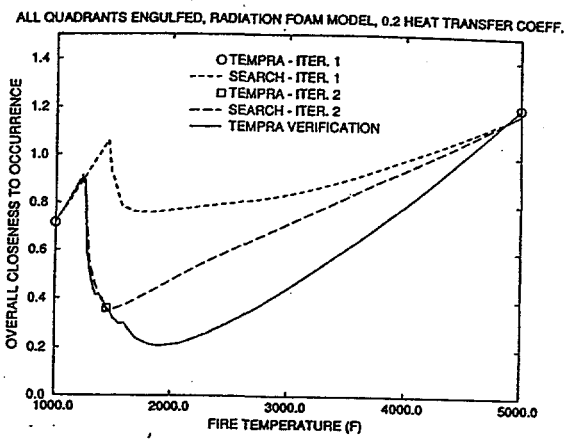

FIGURE 7. VARIATION OF OVERALL CLOSENESS WITH FIRE TEMPERATURE FOR THE FIRST CUT SET: RV CONFIGURATION, CONDITIONS AS INDICATED.

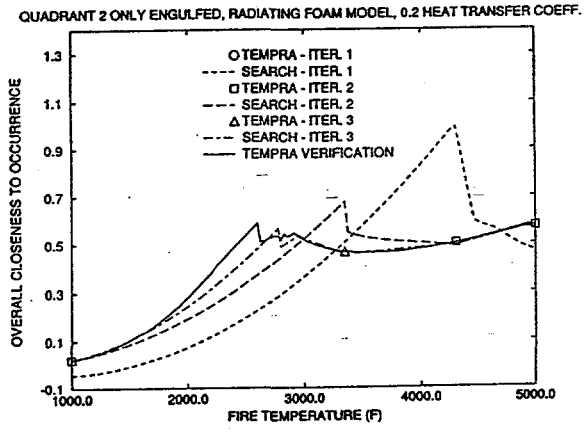

FIGURE 8. VARIATION OF OVERALL CLOSENESS WITH FIRE TEMPERATURE FOR THE 2ND CUT SET: RV CONFIGURATION, CONDITIONS AS INDICATED.

DISCLAIMER